

Published in final edited form as:

*Biochim Biophys Acta*. 2013 September ; 1830(9): 4314–4320. doi:10.1016/j.bbagen.2013.03.033.

## Fibronectin conformation regulates the proangiogenic capability of tumor-associated adipogenic stromal cells

Alwin M. D. Wan<sup>1,2,\*</sup>, Emily M. Chandler<sup>2,\*</sup>, Maya Madhavan<sup>2</sup>, David W. Infanger<sup>2</sup>, Christopher K. Ober<sup>1</sup>, Delphine Gourdon<sup>1</sup>, George G. Malliaras<sup>3</sup>, and Claudia Fischbach<sup>2,4,#</sup>

<sup>1</sup>Department of Materials Science and Engineering, Cornell University, Ithaca, NY 14853, USA

<sup>2</sup>Department of Biomedical Engineering, Cornell University, Ithaca, NY 14853, USA

<sup>3</sup>Department of Bioelectronics, Ecole Nationale Supérieure des Mines, CMP-EMSE, MOC, 880 Route de Mimet, 13541 Gardanne, France

<sup>4</sup>Kavli Institute at Cornell for Nanoscale Science, Cornell University, Ithaca, NY, 14853

### Abstract

**Background**—Changes in fibronectin (Fn) matrix remodeling contribute to mammary tumor angiogenesis and are related to altered behavior of adipogenic stromal cells; yet, the underlying mechanisms remain unclear due in part to a lack of reductionist model systems that allow the inherent complexity of cell-derived extracellular matrices (ECMs) to be deciphered. In particular, breast cancer-associated adipogenic stromal cells not only enhance the composition, quantity, and rigidity of deposited Fn, but also partially unfold these matrices. However, the specific effect of Fn conformation on tumor angiogenesis is undefined.

**Methods**—Decellularized matrices and a conducting polymer device consisting of poly(3,4-ethylenedioxythiophene) doped with poly(styrenesulfonate) (PEDOT:PSS) were used to examine the effect of Fn conformation on the behavior of 3T3-L1 preadipocytes. Changes in cell adhesion and proangiogenic capability were tested via cell counting and by quantification of vascular endothelial growth factor (VEGF) secretion, respectively. Integrin-blocking antibodies were utilized to examine varied integrin specificity as a potential mechanism.

**Results**—Our findings suggest that tumor-associated partial unfolding of Fn decreases adhesion while enhancing VEGF secretion by breast cancer-associated adipogenic precursor cells, and that altered integrin specificity may underlie these changes.

**Conclusions and general significance**—These results not only have important implications for our understanding of tumorigenesis, but also enhance knowledge of cell-ECM interactions that may be harnessed for other applications including advanced tissue engineering approaches.

### Keywords

fibronectin; tumor angiogenesis; integrins; preadipocytes; conducting polymers; bioelectronics

© 2013 Elsevier B.V. All rights reserved.

\*Corresponding Author: Claudia Fischbach-Teschl, Department of Biomedical Engineering, Cornell University, 157 Weill Hall, Ithaca, NY 14853, cf99@cornell.edu, Tel.: +1 (607) 255-4547, Fax: +1 (607) 255-7730.

#These co-authors contributed equally to this work.

**Publisher's Disclaimer:** This is a PDF file of an unedited manuscript that has been accepted for publication. As a service to our customers we are providing this early version of the manuscript. The manuscript will undergo copyediting, typesetting, and review of the resulting proof before it is published in its final citable form. Please note that during the production process errors may be discovered which could affect the content, and all legal disclaimers that apply to the journal pertain.

## 1. Introduction

Sustained angiogenesis represents a hallmark of cancer that is characterized by dynamic changes in extracellular matrix (ECM) remodeling [1]. However, the underlying mechanisms remain unclear due in part to a lack of reductionist model systems that allow the inherent complexity of tumor-associated ECMs to be deciphered. Tumor-associated ECMs develop by aberrant stroma remodeling (i.e., desmoplasia), during which recruited mesenchymal cells (e.g., fibroblasts and adipogenic precursors) deposit increased amounts of a highly fibrillar, crosslinked, and stiff ECM [2,3]. This matrix can directly promote tumor angiogenesis by enhancing transcriptional activity in endothelial cells [4]. Nevertheless, indirect mechanisms may be similarly important, including the stimulated secretion of key proangiogenic molecules (e.g., vascular endothelial growth factor [VEGF]) from the recruited mesenchymal stromal cells [3]. While the characteristic physicochemical properties of the tumor-ECM are commonly attributed to modified collagen synthesis and crosslinking [5], local alterations in the fibronectin (Fn) matrix may be equally involved. In fact, Fn is critical to the formation and turnover of collagen I-based ECMs [6–8] and serves as an indicator for increased tumor aggressiveness [9,10]. Yet, the specific mechanisms by which Fn modulates the proangiogenic capability of tumor-associated stromal cells remain largely undefined.

Fn is a large glycoprotein that contains surface-exposed binding sites for engagement by cell surface receptors (in particular, the RGD loop binding site for multiple integrins), and we have previously shown that in the presence of tumor-derived soluble factors, fibroblasts deposit Fn matrices that are characterized by stretched Fn fibrils and partial molecular unfolding [11]. Cell force-mediated partial unfolding of Fn, in turn, may modulate integrin specificity and thus cell behavior. More specifically, stretching of Fn enhances the distance between RGD-binding and PHSRN synergy sites. This decreases binding specificity of  $\alpha_5\beta_1$  integrins while enhancing engagement of non-synergy-dependent integrins (such as  $\alpha_v\beta_3$  integrins), with potential implications for cellular signaling [12]. Yet, tumor-associated conformational changes of Fn never occur in an isolated manner, but are typically accompanied by simultaneous alterations of Fn matrix quantity and rigidity (Fig. 1) [11,13]. These, in turn, can independently regulate cell behavior, for example, by varying the global density of cell binding motifs and activating cell contractility-dependent signaling cascades, respectively [14,15]. A variety of experimental platforms have been developed to study cell behavior as a function of adhesion peptide density and ECM mechanical properties, including RGD-modified hydrogel systems and polyacrylamide gels of varying stiffness, respectively [14,16,17]. Additionally, biomaterials systems with engineered integrin-specific ECM fragments permit interrogating the role of integrin binding specificity on cellular outcomes [18–20]. Nevertheless, culture models to independently investigate the role of full length Fn conformation on cell behaviors have been limited.

Here, we utilized a previously developed conducting polymer device to study the role of Fn conformation on the proangiogenic capability of tumor-associated stromal cells, independent of varied ECM quantity, composition, and stiffness (Fig. 1) [21–23]. This device consists of thin films of poly(3,4-ethylenedioxythiophene) doped with poly(styrenesulfonate) (PEDOT:PSS) and permits electrical control of adsorbed Fn molecular conformation in cell culture [23]. Our findings suggest that Fn conformation regulates proangiogenic factor secretion in tumors via altered integrin specificity, and stresses the suitability of conducting polymers in evaluating the underlying molecular mechanisms.

## 2. Materials and Methods

### 2.1 Cell culture

3T3-L1 murine preadipocytes and MDA-MB231 human breast cancer cells (both from ATCC) were routinely cultured in MEM ( $\alpha$ -modification [ $\alpha$ -MEM], Sigma-Aldrich) containing 10% fetal bovine serum (FBS, Tissue Culture Biologicals) and 1% penicillin/streptomycin (pen/strep) (Invitrogen); 3T3-L1s were used up to passage ten. Human bone marrow-derived mesenchymal stem cells (MSCs) were acquired from Lonza and maintained in MSC-GM (Lonza). To induce tumor-associated stromal cell behavior, 3T3-L1s were cultured in tumor conditioned media (TCM) as previously described [3,11]. Briefly, TCM was collected from MDA-MB231 cells 24 hours after addition of  $\alpha$ -MEM containing 1% FBS and pen/strep, normalized to cell number, concentrated 10-fold, and reconstituted with fresh  $\alpha$ -MEM/1% FBS/pen/strep to a final 2-fold concentration. Control media was incubated and concentrated in a manner similar to TCM. The pUR4 peptide inhibiting Fn polymerization and the Del29 control peptide were kindly provided by J. Sottile [24] and supplemented at 500 nM at the time of seeding and all subsequent media changes.

### 2.2 Generation and characterization of decellularized matrices and VEGF analysis

To generate control and tumor-mimetic ECMs (hereby referred to as tumor ECMs), previously published methods were used [3,25]. Briefly, 3T3-L1 cells were seeded onto gelatin (Fisher Scientific)-coated 12-well dishes at a density of 3,000 cells/cm<sup>2</sup> and cultured in control media or TCM (both supplemented with 50  $\mu$ g/mL ascorbic acid [Sigma-Aldrich]) that were changed every other day. On day 8, decellularized matrices were generated by extracting cells through digestion in a solution of 20 mM NH<sub>4</sub>OH and 0.5% Triton-X (both from VWR) in phosphate buffered saline (PBS, HyClone) followed by thorough washing in water and PBS. To detect differences in Fn, immunofluorescent staining of the decellularized matrices was performed with a primary antibody raised against Fn (Sigma-Aldrich), an Alexa Fluor 488-labelled secondary antibody, and DAPI (both from Invitrogen) to confirm absence of cells. To analyze varied adhesion and VEGF secretion, new 3T3-L1 cells (7,000 cells/cm<sup>2</sup>) were seeded atop the decellularized matrices in serum-free  $\alpha$ -MEM. After 24 hours, media was collected and analyzed via Quantikine mouse VEGF ELISA (R&D Systems). VEGF content was normalized to cell numbers as counted on a Beckman Z2 Particle Analyzer following trypsinization. Additionally, lysates of decellularized matrices were analyzed via ELISA to assess potential differences in VEGF binding to the different matrices. For analysis of VEGF transcription, total RNA was harvested by Trizol extraction (Invitrogen). RNA was quantified using a Nanodrop 2000 spectrophotometer (Thermo Scientific); 1 $\mu$ g total RNA was reverse transcribed to cDNA using qScript cDNA supermix (random hexamer and oligo-dT primers, Quanta Biosciences). For real-time, RT PCR, 25 ng of cDNA template was run for each sample in duplicate using SYBR-based detection (Quanta PerfeCTa® SYBR® Green FastMix®, Low ROX) and standard PCR conditions, performed on an Applied Biosystems 7500 real-time PCR system. Primer sequences for mouse VEGF and beta-actin were designed and synthesized (IDT Technologies), and subsequently validated for efficiency and specificity prior to use. Sequences were as follows: mouse VEGF forward 5'-CTTGTTTCAGAGCGGAGAAAGC-3', Reverse 5'-ACATCTGCAAGTACGTTTCGTT-3'; mouse beta-actin 5'-CATCCTCTTCCTCCCTGGAGAAGA-3', Reverse 5'-ACAGGATTCCATACCCAAGAAGGAAG-3'. Data were analyzed using the comparative c(T) method [26] and normalized to control (untreated) VEGF expression.

### 2.3 Evaluation of endothelial cell behavior

Human umbilical vein endothelial cells (HUVECs, Lonza) were maintained in endothelial growth medium (EGM-2, Lonza) and utilized to assess the relevance of ECM-dependent

stroma proangiogenic capability. Specifically, 3T3-L1 cells were cultured on control and tumor ECMs for 24 hours, after which media was collected. This media was normalized to cell number, concentrated 10-fold, diluted 1:1 in EGM-2 without growth factors, and utilized for HUVEC transwell migration assays. To this end, sterile transwells (BD Fluoro-Block, 8.0 $\mu$ m membrane) were coated with 20  $\mu$ g/mL PureCol<sup>®</sup> collagen I (Inamed) in PBS, placed in wells containing 3T3-L1 conditioned media from control or tumor ECMs, and seeded with HUVECs at a concentration of 60,000 cells/mL. For blocking VEGF signaling, HUVECs were incubated with 5  $\mu$ g/ml VEGF-R2 heptapeptide antagonist (Anaspec). Transwell migration assays were performed for 24 hours, after which cells were fixed in formalin (EMD). The upper part of the membranes were swabbed to remove non-migrated cells, and cell nuclei were stained with 4',6-diamidino-2-phenylindole (DAPI, Invitrogen), imaged on a Zeiss Observer Z.1 microscope with an AxioCam MRm camera, and quantified by image analysis with ImageJ (NIH).

#### 2.4 Conducting polymer devices to evaluate the effect of Fn conformation on stromal cells

Conducting polymer devices to control Fn conformation were fabricated by patterning poly(3,4-ethylenedioxythiophene) (PEDOT:PSS) thin films on glass substrates, and subsequently attaching polydimethylsiloxane (PDMS) fluid reservoirs (Fig. 1, bottom). Specifically, 20 mL of PEDOT:PSS aqueous dispersion (Heraeus Clevis<sup>™</sup> PH 1000) were mixed with 5 mL of ethylene glycol, 50  $\mu$ L of dodecyl benzene sulfonic acid (DBSA), and 1 wt% of 3-glycidoxypropyltrimethoxysilane (GOPS, as a cross-linker). The resulting dispersion was spin-coated on cleaned glass slides (with tape lift-off masks to pattern the PEDOT:PSS into two macroscopic pixels). The films were baked at 140°C for 1 hour, and then immersed in PBS for several hours to remove excess low molecular weight compounds. PDMS reservoirs with two chambers (i.e., one over each PEDOT:PSS pixel) were treated with UV-ozone and subsequently manually adhered to the glass/PEDOT:PSS devices. Prior to cell seeding, the devices were sterilized in 70% ethanol, thoroughly washed, and subsequently coated with serum or Fn by adding  $\alpha$ -MEM/1% pen/strep containing either 10% FBS or 30  $\mu$ g/mL Fn, respectively, to the PDMS fluid reservoirs. Concomitantly, a bipolar power supply sourced +1.0 V and -1.0 V to the two PEDOT:PSS pixels of each device for 1 hour to control the conformation of adsorbed Fn. After rinsing in PBS, 3T3-L1s or MSCs were seeded; following their adhesion, media was changed to  $\alpha$ -MEM containing 1% FBS and pen/strep or serum free MSC-GM, respectively, and collected after 24 hours at which point cells were fixed in formalin (EMD). Cell nuclei were stained with DAPI and quantified as described above. VEGF secretion was analyzed via Quantikine mouse VEGF ELISA for 3T3-L1s or human VEGF ELISA for hMSCs (both from R&D Systems) and normalized to the number of cell nuclei. For VEGF-binding studies, cell-free devices were incubated with 150 pg/mL human recombinant VEGF (based on cell-secreted amounts; R&D Systems) for 2 hours in the same media that was utilized for secretion studies. Subsequently, media was removed and analyzed using a human VEGF ELISA (R&D Systems). For studies involving integrin inhibition, cells were incubated for 30 minutes with anti- $\beta$ <sub>1</sub> (R&D Systems) and anti- $\alpha$ <sub>v</sub> (Millipore) function-blocking antibody prior to seeding.

#### 2.5 Statistical analysis

Statistical analysis was performed using GraphPad Prism 5. Student's *t* tests were used to compare pairs of data sets, and a p-value of less than 0.05 was considered statistically significant. Data are represented as average  $\pm$  standard deviation of at least 3 independent experiments.

### 3. Results and Discussion

#### 3.1 Tumor stromal cell-derived matrices modulate stromal cell proangiogenic capability

We previously reported that tumor-derived soluble factors induce adipogenic precursor cells to (i) self-stimulate their proangiogenic capability in an ECM-dependent manner [3] and (ii) elevate Fn matrix deposition [11]. However, it remains unclear whether or not altered Fn matrix assembly directly contributes to the increased proangiogenic potential of tumor-associated adipogenic precursors. To investigate this possible functional link, we first evaluated the effect of ECMs deposited by control and tumor-associated adipogenic stromal cells on the behavior of native adipogenic precursors. To this end, 3T3-L1 preadipocytes were cultured in TCM and control media followed by detergent-based decellularization as previously reported [3]. Immunostaining of these matrices confirmed our ability to generate cell-free, tumor-mimicking matrices, characterized by increased levels of fibrillar Fn (Fig. 2A) that is partially unfolded [11] relative to the control matrices. Interestingly, reseeding and analysis of new 3T3-L1s onto these matrices revealed that tumor-conditioned matrices inhibited adhesion (30%) relative to control ECMs (Fig. 2B), whereas VEGF secretion per cell was enhanced (47%) in the tumor relative to the control condition (Fig. 2C). Different VEGF levels were related to altered VEGF synthesis rather than differential VEGF sequestration in the matrices; control and tumor-conditioned matrices contained only negligible amounts of VEGF (approx. 8% of VEGF measured in the media) that were not significantly different between conditions (Fig. 2D) and VEGF mRNA levels of cells cultured on tumor-conditioned matrices were greater (59%) relative to cells on control ECMs. These data suggest that Fn matrix content/conformation and stromal cell VEGF secretion may be correlated. However, as decellularized matrices contain various other ECM molecules including collagen I and proteoglycans [27], we next performed experiments to more directly confirm the contribution of Fn to the observed changes. We produced decellularized matrices devoid of Fn fibrils using pUR4, a peptide capable of blocking Fn polymerization [28]. Indeed, addition of pUR4 inhibited Fn incorporation into the TCM-treated stromal cell matrices (Fig. 3A), which increased adhesion (Fig. 3B) and decreased VEGF secretion (Fig. 3C) of reseeded 3T3-L1s to levels comparable to control matrices. While these experiments confirm that Fn regulates the adhesive and proangiogenic ability of stromal cells observed with decellularized matrices we note that blockade of Fn matrix assembly may interfere with deposition of other ECM components including collagen [29], and it is possible that these changes partially contribute to our results.

To determine the functional relevance of stromal cell secretory changes to endothelial cell behavior, we collected media from 3T3-L1 cells cultured on control and tumor ECMs, and studied their effect on HUVEC migration via a transwell assay. Corresponding with the previously detected increased VEGF levels, HUVEC migration was significantly elevated in the presence of media collected from tumor-conditioned ECM cultures (Fig. 4A). To further verify that these differences in HUVEC migration were related to tumor ECM-induced changes of VEGF secretion rather than other factors, we conducted another control experiment in which we repeated the HUVEC migration assay with 3T3-L1-conditioned media from tumor-mimicking ECM in the presence and absence of a VEGF signaling inhibitor. For these experiments, HUVECs were incubated with an antagonist that prevents binding of VEGF to its main receptor VEGFR2/KDR, which activates downstream signaling cascades primarily responsible for changes in angiogenesis [30]. VEGF blockade significantly reduced HUVEC migration (20%) in response to 3T3-L1 conditioned media collected from tumor ECM cultures (Fig. 4B). Nevertheless, other secreted factors including proangiogenic molecules such as basic fibroblast growth factor or soluble Fn [31,32] may also play a role, and likely account for the difference in endothelial cell migration between control and VEGF-inhibited conditions.

### 3.2 Fn conformation regulates stromal cell proangiogenic signaling

As treatment of 3T3-L1 cells with TCM leads to ECM-incorporation of Fn in partially unfolded conformations [11], and because Fn conformational changes can alter cell behavior via regulating integrin specificity [12,18], we hypothesized that Fn conformational state may be instrumental to the pro-angiogenic function of stromal cells. To investigate this hypothesis, we sought to isolate the effect of Fn conformation from other potential variations in the ECM (e.g., composition, quantity, density, rigidity) with the use of a previously established conducting polymer device [21–23]. This device consists of PEDOT:PSS-coated culture chambers capable of establishing over a large area, any single conformation (or range of conformations) of adsorbed Fn from compact, to extended, to partially unfolded. Further, this level of control over conformation can be achieved without modification of overall mechanical stiffness or biochemistry (i.e., composition) that occur in native ECMs [23].

Devices were first coated with Fn in serum-free media for one hour under an applied bias of +1 V and –1 V to establish Fn in compact and unfolded conformations, respectively. 3T3-L1s were then seeded on the prepared surfaces and their changes in adhesion as well as VEGF secretion were measured as a function of Fn conformation. Our data indicate that 20% fewer cells adhered to unfolded Fn as compared to compact Fn (Fig. 5A) and that cells cultured on surfaces with unfolded Fn secreted 40% more VEGF than cells cultured on compact Fn (Fig. 5B), suggesting that the changes in adhesion and pro-angiogenic capability observed with decellularized matrices may be linked to changes in Fn conformation. In fact, tumor-associated ECMs comprise a large ensemble of molecular Fn conformations (including unfolded states) [11], and relaxed conformations may occur even in highly-strained fibers [33], which makes the relatively large differences in adhesion and VEGF secretion found on decellularized matrices seem even more dramatic.

We next repeated these experiments with serum-containing media (10% FBS), which regulates cell adhesion on our devices in a Fn conformation-dependent manner [21], while also enabling us to test the relevance of our findings under more physiologically relevant conditions. More specifically, body fluids such as serum not only contain soluble Fn, but also numerous other proteins (e.g., additional ECM molecules, growth factors). These other proteins bind to Fn in a conformation-dependent manner, and could thus modulate cell response to Fn conformation [34]. We observed that 40% fewer cells adhered to cultures representative of unfolded Fn as compared to compact Fn (Fig. 5A), whereas unfolded Fn promoted VEGF secretion (65%) relative to compact Fn (Fig. 5B). These changes in soluble VEGF were related to altered secretion, rather than conformation-dependent binding of VEGF to adsorbed Fn. Specifically, VEGF binding studies with cell-free devices confirmed that unfolded Fn promotes interactions with VEGF, likely via exposing cryptic binding sites (Fig. 6A) [35,36]. To further demonstrate the broad relevance of our findings we investigated the effect of Fn conformation on bone marrow-derived human mesenchymal stem cells (hMSCs), a cell type that is recruited by tumors *in vivo* [37] and widely utilized in tissue engineering applications including therapeutic angiogenesis [38]. MSCs similarly exhibited increased (140%) VEGF secretion in response to unfolded Fn conformation (Fig. 6B) underlining that our results are not limited to the utilized murine 3T3-L1 cell line, but have relevance to other cell types, including human primary cells.

### 3.3 Fn conformation regulates proangiogenic stromal cell signaling via altering integrin specificity

Partial unfolding of Fn can alter cell behavior via modulating binding specificity of synergy-dependent (e.g.,  $\alpha_5\beta_1$ ) and non-synergy-dependent integrins (e.g.,  $\alpha_v\beta_3$ ) [12,39,40]. Therefore, we hypothesized that the detected differences in stromal cell proangiogenic factor

secretion are related to Fn-conformation-dependent variations in  $\alpha_5\beta_1$  and  $\alpha_v\beta_3$  engagement. Specifically,  $\alpha_5\beta_1$  integrins simultaneously bind PHSRN and RGD sequences on the neighboring III<sub>9</sub> and III<sub>10</sub> modules of Fn, respectively [41]. As a result, Fn extension progressively inhibits  $\alpha_5\beta_1$  binding by increasing the spatial separation between the RGD and synergy sites [12]. In these situations, cells may utilize more  $\alpha_v\beta_3$  integrins for binding, to compensate for the reduced engagement of  $\alpha_5\beta_1$  integrins [39], which may, in turn, elevate VEGF secretion [42].

To investigate the relevance of these connections to our findings, we first tested the role of  $\alpha_5\beta_1$  in regulating cellular VEGF secretion on compact Fn. We inhibited  $\alpha_5\beta_1$  by incubating 3T3-L1s with a  $\beta_1$  function-blocking antibody prior to seeding onto devices with compact Fn. These experiments were performed over 24 hours, a time frame during which we observed no deposition of collagen type I matrices (data not shown). With this approach we reduced the likelihood that inhibition of other  $\beta_1$ -dependent integrins (such as  $\alpha_2\beta_1$ ) obscured our results [19]. Interestingly, blockade of  $\beta_1$  stimulated VEGF secretion relative to the no antibody-control condition, suggesting that  $\alpha_5\beta_1$ -mediated interactions with compact Fn may contribute to decreased VEGF secretion by stromal cells (Fig. 7, white bars). This effect was inhibited by simultaneous addition of an  $\alpha_v$  function-blocking antibody, indicating that compensatory  $\alpha_v\beta_3$  may play a role in this process. Next, we tested the contribution of  $\alpha_v\beta_3$  to increased VEGF secretion of cells interacting with partially unfolded Fn. Addition of an  $\alpha_v$  function-blocking antibody to cultures on partially unfolded Fn decreased VEGF secretion to similar levels as detected with cultures on compact Fn (Fig. 7, black bars). In support of our hypothesis, concomitant inhibition of  $\alpha_5\beta_1$  had no effect, likely due to intrinsically reduced levels of  $\alpha_5\beta_1$  binding to partially unfolded Fn. Together, these results suggest that partial Fn unfolding enhances VEGF secretion in tumor-associated matrices by favoring  $\alpha_v\beta_3$  over  $\alpha_5\beta_1$  engagement, in agreement with studies by others showing that increased engagement of  $\alpha_v\beta_3$  promotes VEGF secretion [42]. Nevertheless, this effect may be further modulated by the physicochemical complexity of the tumor ECM that not only entails spatial differences in Fn conformation [11,33], but also varied composition, quantity and rigidity, which can all regulate the observed integrin switching effect. In the future, biologically-inspired biomaterials (e.g., non-adhesive materials functionalized with recombinant Fn fragments) specifically designed to dissect the contribution of integrin specificity to cellular activities may help to further decipher the role of Fn conformation in altering stromal cell behavior [20,39].

## 5. Summary and conclusions

While our previous work has suggested that tumor stromal cells deposit partially unfolded Fn [8], we now link these changes to increased proangiogenic capacity of these cells with implications for tumor angiogenesis. Collectively, our findings suggest that Fn conformation regulates cell signaling independent of other variables typically associated with altered ECM deposition (e.g., composition, quantity, rigidity), and that variations in integrin binding specificity may contribute to this. While our studies were specifically designed to evaluate stromal cell behavior, other cell types composing the tumor microenvironment (e.g., tumor cells themselves, endothelial cells, immune cells) may be similarly responding to Fn conformational changes and should be evaluated in future studies. One challenge with our approach includes that cell-ECM interactions can vary between 2-D and 3-D culture formats, which may affect signaling in response to altered Fn conformation [43,44]. Utilization of conducting 3-D polymer scaffolds rather than thin films may help to address this possibility and are currently being developed by our groups. Finally, our results have broad implications for the field of tissue engineering: Fn adsorption to implanted devices is widely known to result in conformational changes, which may influence integration, foreign body response, and functionality of these devices [45,46]. Studying the underlying cellular

signaling with conducting polymers will help to improve our understanding of cell-biomaterial interactions and expand our ability to harness those interactions for improved tissue engineering approaches.

## Acknowledgments

Funding was provided by the National Science Foundation through a graduate research fellowship for E. Chandler and a Biology Undergraduate Research Fellowship for M. Madhavan, the Partner University Fund (a program of French American Cultural Exchange) as well as the National Cancer Institute (RC1CA146065, R21CA161532, and by the Cornell Center on the Microenvironment & Metastasis through Award Number U54CA143876). D.W. Infanger was supported by a basic research fellowship from the American Brain Tumour Association. The content is solely the responsibility of the authors and does not necessarily represent the official views of the National Cancer Institute or the National Institutes of Health.

## References

- Hanahan D, Weinberg RA. Hallmarks of cancer: the next generation. *Cell*. 2011; 144:646–74. [PubMed: 21376230]
- Kalluri R, Zeisberg M. Fibroblasts in cancer. *Nature Reviews: Cancer*. 2006; 6:392–401.
- Chandler EM, Seo BR, Califano JP, Andresen Eguiluz RC, Lee JS, Yoon CJ, Tims DT, Wang JX, Cheng L, Mohanan S, Buckley MR, Cohen I, Nikitin AY, Williams RM, Gourdon D, Reinhart-King CA, Fischbach C. Implanted adipose progenitor cells as physicochemical regulators of breast cancer. *Proceedings of the National Academy of Sciences of the United States of America*. 2012; 109:9786–91. [PubMed: 22665775]
- Mammoto A, Connor KM, Mammoto T, Yung CW, Huh D, Aderman CM, Mostoslavsky G, Smith LEH, Ingber DE. A mechanosensitive transcriptional mechanism that controls angiogenesis. *Nature*. 2009; 457:1103–8. [PubMed: 19242469]
- Levental KR, Yu H, Kass L, Lakins JN, Egeblad M, Erler JT, Fong SFT, Csiszar K, Giaccia A, Weninger W, Yamauchi M, Gasser DL, Weaver VM. Matrix crosslinking forces tumor progression by enhancing integrin signaling. *Cell*. 2009; 139:891–906. [PubMed: 19931152]
- Anderson JM. Biological Responses to Materials. *Annual Review of Materials Research*. 2001; 31:81–110.
- Midwood KS, Williams LV, Schwarzbauer JE. Tissue repair and the dynamics of the extracellular matrix. *The International Journal of Biochemistry & Cell Biology*. 2004; 36:1031–7.
- Welch MP. Temporal relationships of F-actin bundle formation, collagen and fibronectin matrix assembly, and fibronectin receptor expression to wound contraction. *The Journal of Cell Biology*. 1990; 110:133–145. [PubMed: 2136860]
- Sethi T, Rintoul RC, Moore SM, MacKinnon AC, Salter D, Choo C, Chilvers ER, Dransfield I, Donnelly SC, Strieter R, Haslett C. Extracellular matrix proteins protect small cell lung cancer cells against apoptosis: a mechanism for small cell lung cancer growth and drug resistance in vivo. *Nature Medicine*. 1999; 5:662–8.
- Zhang Y, Lu H, Dazin P, Kapila Y. Squamous cell carcinoma cell aggregates escape suspension-induced, p53-mediated anoikis: fibronectin and integrin  $\alpha_v$  mediate survival signals through focal adhesion kinase. *The Journal of Biological Chemistry*. 2004; 279:48342–9. [PubMed: 15331608]
- Chandler EM, Saunders MP, Yoon CJ, Gourdon D, Fischbach C. Adipose progenitor cells increase fibronectin matrix strain and unfolding in breast tumors. *Physical Biology*. 2011; 8:015008. [PubMed: 21301062]
- Krammer A, Craig D, Thomas WE, Schulten K, Vogel V. A structural model for force regulated integrin binding to fibronectin's RGD-synergy site. *Matrix Biology*. 2002; 21:139–147. [PubMed: 11852230]
- Klotzsch E, Smith ML, Kubow KE, Muntwyler S, Little WC, Beyeler F, Gourdon D, Nelson BJ, Vogel V. Fibronectin forms the most extensible biological fibers displaying switchable force-exposed cryptic binding sites. *Proceedings of the National Academy of Sciences*. 2009; 106:18267–18272.



14. Hsiong SX, Huebsch N, Fischbach C, Kong HJ, Mooney DJ. Integrin-adhesion ligand bond formation of preosteoblasts and stem cells in three-dimensional RGD presenting matrices. *Biomacromolecules*. 2008; 9:1843–51. [PubMed: 18540674]
15. DuFort CC, Paszek MJ, Weaver VM. Balancing forces: architectural control of mechanotransduction. *Nature Reviews Molecular Cell Biology*. 2011; 12:308–19.
16. Schwartzman M, Palma M, Sable J, Abramson J, Hu X, Sheetz MP, Wind SJ. Nanolithographic control of the spatial organization of cellular adhesion receptors at the single-molecule level. *Nano Letters*. 2011; 11:1306–12. [PubMed: 21319842]
17. Wang, Y-L.; RJP. *Methods in Enzymology*. Elsevier; 1998. Preparation of a flexible, porous polyacrylamide substrate for mechanical studies of cultured cells.
18. Grant RP, Spitzfaden C, Altroff H, Campbell ID, Mardon HJ. Structural requirements for biological activity of the ninth and tenth FIII domains of human fibronectin. *The Journal of Biological Chemistry*. 1997; 272:6159–66. [PubMed: 9045628]
19. Reyes CD, Petrie TA, García AJ. Mixed extracellular matrix ligands synergistically modulate integrin adhesion and signaling. *Journal of Cellular Physiology*. 2008; 217:450–8. [PubMed: 18613064]
20. Martino MM, Mochizuki M, Rothenfluh DA, Rempel SA, Hubbell JA, Barker TH. Controlling integrin specificity and stem cell differentiation in 2D and 3D environments through regulation of fibronectin domain stability. *Biomaterials*. 2009; 30:1089–97. [PubMed: 19027948]
21. Wan AMD, Brooks DJ, Gumus A, Fischbach C, Malliaras GG. Electrical control of cell density gradients on a conducting polymer surface. *Chemical Communications*. 2009:5278–80. [PubMed: 19707645]
22. Gumus A, Califano JP, Wan AMD, Huynh J, Reinhart-King CA, Malliaras GG. Control of cell migration using a conducting polymer device. *Soft Matter*. 2010; 6:5138.
23. Wan AMD, Schur RM, Ober CK, Fischbach C, Gourdon D, Malliaras GG. Electrical control of protein conformation. *Advanced Materials*. 2012; 24:2501–2505. [PubMed: 22489011]
24. Tomasini-Johansson BR, Kaufman NR, Ensenberger MG, Ozeri V, Hanski E, Mosher DF. A 49-residue peptide from adhesin F1 of *Streptococcus pyogenes* inhibits fibronectin matrix assembly. *The Journal of Biological Chemistry*. 2001; 276:23430–9. [PubMed: 11323441]
25. Beacham DA, Amatangelo MD, Cukierman E. Preparation of extracellular matrices produced by cultured and primary fibroblasts. *Current Protocols in Cell Biology*. 2007; 33:10.9.1–10.9.21.
26. Schmittgen TD, Livak KJ. Analyzing real-time PCR data by the comparative CT method. *Nature Protocols*. 2008; 3:1101–1108.
27. Amatangelo MD, Bassi DE, Klein-Szanto AJP, Cukierman E. Stroma-derived three-dimensional matrices are necessary and sufficient to promote desmoplastic differentiation of normal fibroblasts. *The American Journal of Pathology*. 2005; 167:475–88. [PubMed: 16049333]
28. Ozeri V, Tovi A, Burstein I, Natanson-Yaron S, Caparon MG, Yamada KM, Akiyama SK, Vlodavsky I, Hanski E. A two-domain mechanism for group A streptococcal adherence through protein F to the extracellular matrix. *The EMBO Journal*. 1996; 15:989–98. [PubMed: 8605894]
29. Sottile J, Hocking DC. Fibronectin polymerization regulates the composition and stability of extracellular matrix fibrils and cell-matrix adhesions. *Molecular Biology of the Cell*. 2002; 13:3546–59. [PubMed: 12388756]
30. Cross MJ, Dixelius J, Matsumoto T, Claesson-Welsh L. VEGF-receptor signal transduction. *Trends in Biochemical Sciences*. 2003; 28:488–94. [PubMed: 13678960]
31. Fischbach C, Mooney DJ. Polymers for pro- and anti-angiogenic therapy. *Biomaterials*. 2007; 28:2069–76. [PubMed: 17254631]
32. Zhou X, Rowe RG, Hiraoka N, George JP, Wirtz D, Mosher DF, Virtanen I, Chernousov MA, Weiss SJ. Fibronectin fibrillogenesis regulates three-dimensional neovessel formation. *Genes & Development*. 2008; 22:1231–43. [PubMed: 18451110]
33. Bradshaw MJ, Smith ML. Contribution of unfolding and intermolecular architecture to fibronectin fiber extensibility. *Biophysical Journal*. 2011; 101:1740–8. [PubMed: 21961600]
34. Singh P, Carraher C, Schwarzbauer JE. Assembly of fibronectin extracellular matrix. *Annual Review of Cell and Developmental Biology*. 2010; 26:397–419.

35. Mitsi M, Hong Z, Costello CE, Nugent MA. Heparin-mediated conformational changes in fibronectin expose vascular endothelial growth factor binding sites. *Biochemistry*. 2006; 45:10319–28. [PubMed: 16922507]
36. Mitsi M, Forsten-Williams K, Gopalakrishnan M, Nugent MA. A catalytic role of heparin within the extracellular matrix. *The Journal of Biological Chemistry*. 2008; 283:34796–807. [PubMed: 18845539]
37. Karnoub AE, Dash AB, Vo AP, Sullivan A, Brooks MW, Bell GW, Richardson AL, Polyak K, Tubo R, Weinberg RA. Mesenchymal stem cells within tumour stroma promote breast cancer metastasis. *Nature*. 2007; 449:557–63. [PubMed: 17914389]
38. Grainger SJ, Carrion B, Ceccarelli J, Putnam A. Stromal Cell Identity Influences the In Vivo Functionality of Engineered Capillary Networks Formed by Co-Delivery of Endothelial Cells and Stromal Cells. *Tissue Engineering, Part A*. 2012 [Epub, ahead of print].
39. Petrie TA, Capadona JR, Reyes CD, García AJ. Integrin specificity and enhanced cellular activities associated with surfaces presenting a recombinant fibronectin fragment compared to RGD supports. *Biomaterials*. 2006; 27:5459–70. [PubMed: 16846640]
40. Friedland JC, Lee MH, Boettiger D. Mechanically activated integrin switch controls alpha5beta1 function. *Science*. 2009; 323:642–4. [PubMed: 19179533]
41. Pierschbacher MD, Ruoslahti E. Cell attachment activity of fibronectin can be duplicated by small synthetic fragments of the molecule. *Nature*. 1984; 309:30–33. [PubMed: 6325925]
42. De S, Razorenova O, McCabe NP, O'Toole T, Qin J, Byzova TV. VEGF-integrin interplay controls tumor growth and vascularization. *Proceedings of the National Academy of Sciences of the United States of America*. 2005; 102:7589–94. [PubMed: 15897451]
43. Fischbach C, Kong HJ, Hsiong SX, Evangelista MB, Yuen W, Mooney DJ. Cancer cell angiogenic capability is regulated by 3D culture and integrin engagement. *Proceedings of the National Academy of Sciences of the United States of America*. 2009; 106:399–404. [PubMed: 19126683]
44. Fraley SI, Feng Y, Krishnamurthy R, Kim DH, Celedon A, Longmore GD, Wirtz D. A distinctive role for focal adhesion proteins in three-dimensional cell motility. *Nature Cell Biology*. 2010; 12:598–604.
45. Dolatshahi-Pirouz A, Jensen T, Foss M, Chevallier J, Besenbacher F. Enhanced surface activation of fibronectin upon adsorption on hydroxyapatite. *Langmuir*. 2009; 25:2971–8. [PubMed: 19437707]
46. Kao WJ, Lee D, Schense JC, Hubbell JA. Fibronectin modulates macrophage adhesion and FBGC formation: The role of RGD, PHSRN, and PRRARV domains. *Journal of Biomedical Materials Research*. 2001; 55:79–88. [PubMed: 11426401]

### Highlights

- We study effects of tumor-associated fibronectin (Fn) on adipogenic stromal cells.
- Decellularized matrices allow examining global effects of Fn.
- Conducting polymers enable isolated control over Fn conformation.
- Fn unfolding decreases adhesion while increasing proangiogenic factor secretion.
- Fn conformation modulates cellular behavior via changing integrin specificity.

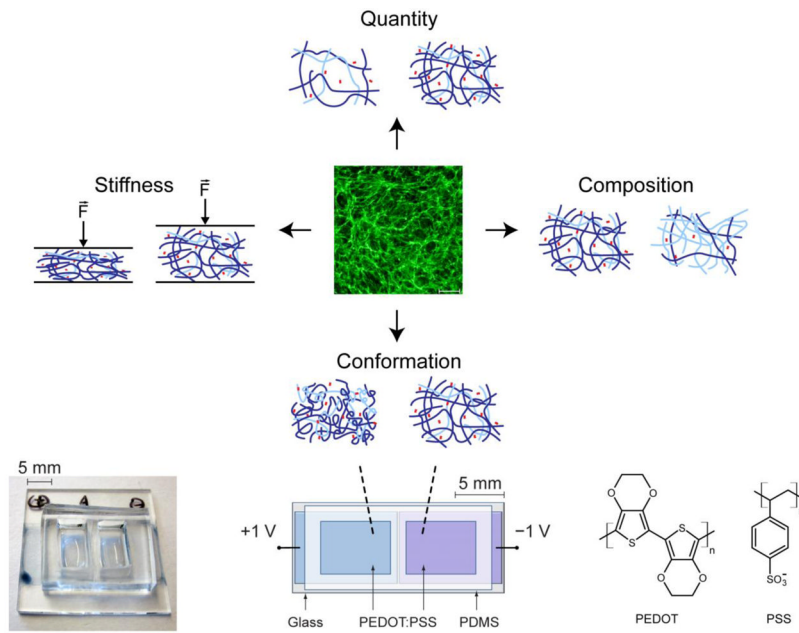


**Figure 1. Conducting polymers enable control over Fn conformation**

In the presence of tumor-derived soluble factors, adipogenic stromal cells deposit ECMs that vary with regard to quantity, composition, mechanical properties, and conformation of component proteins including Fn. While a variety of approaches have been developed to study the isolated effects of ECM quantity, composition, and stiffness, there is a lack of culture models for investigating cell behavior in response to specific ECM conformations. Conducting polymer devices made from thin film pixels of PEDOT:PSS overcome this shortcoming and permit control over Fn conformation in isolation [23], enabling studies of how changes in Fn conformation direct cell responses.

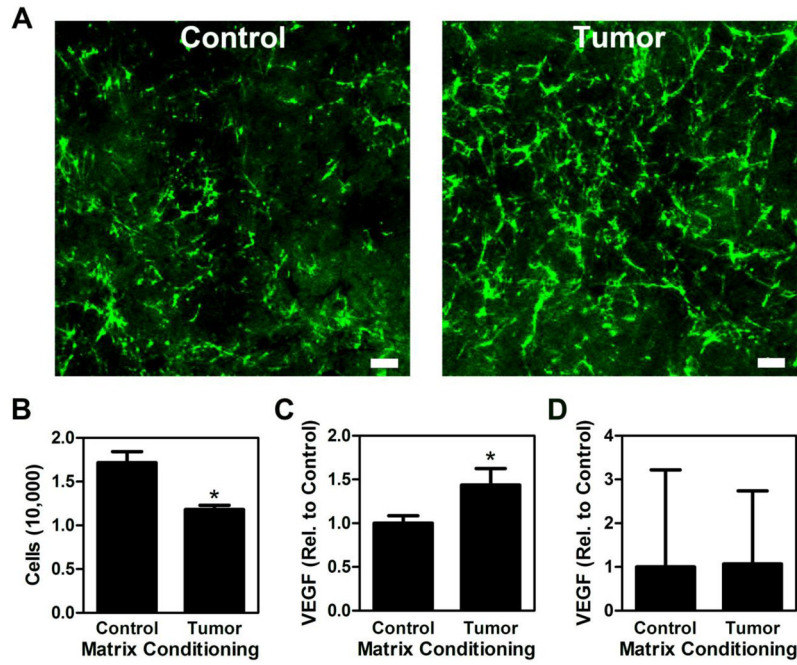


**Figure 2. Decellularized tumor-associated matrices influence adipogenic stromal cell adhesion and proangiogenic factor secretion**

3T3-L1 cells assemble a denser, more fibrillar matrix with increased Fn content when cultured in the presence of TCM [11], which was reflected with decellularized matrices prepared from control (Control) and TCM-treated 3T3-L1s (Tumor) using detergent-based methods. Scale bar = 20  $\mu\text{m}$  (A). Tumor matrices decreased the total number of adherent 3T3-L1 per well as determined by counting trypsinized cells (B) and increased VEGF secretion per cell as analyzed via ELISA followed by normalization to cell number (C). Varied VEGF levels were not due to differential ECM sequestration because ELISA of lysates of decellularized ECMs did not reveal statistically significant differences between conditions (D). \* indicates  $p < 0.05$ .

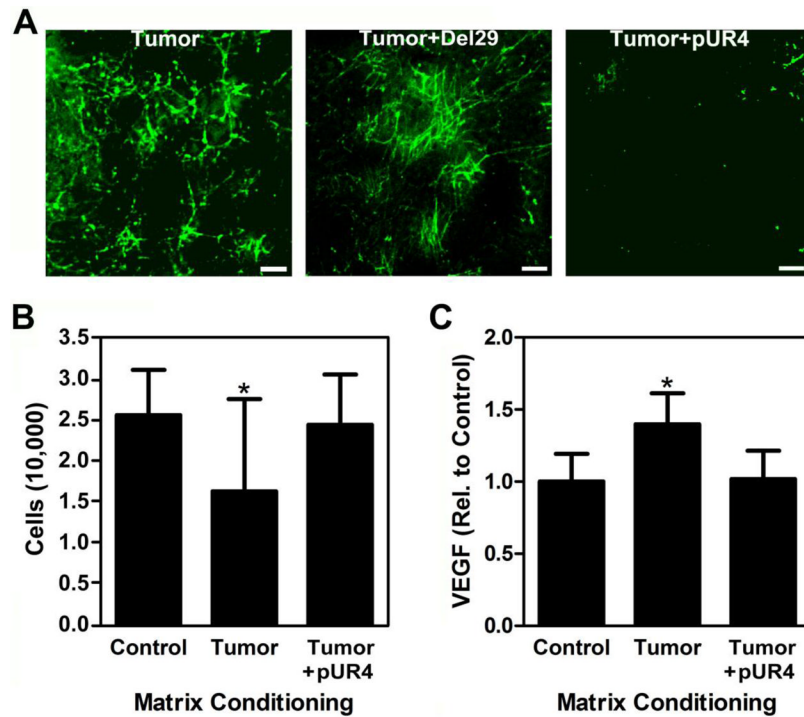


**Figure 3. Fn influences cell behavior in response to control and tumor ECMs**

Addition of the control peptide Del29 during preparation of tumor ECMs does not alter Fn incorporation, whereas addition of the Fn polymerization inhibitor pUR4 markedly decreased Fn incorporation. Scale bar = 20  $\mu$ m (A). Accordingly, tumor matrices prepared in the presence of pUR4 increased cell adhesion as determined by counting of trypsinized cells (B) and diminished VEGF secretion as analyzed via ELISA followed by normalization to cell number (C) to levels comparable to control matrices. \* indicates  $p < 0.05$ .

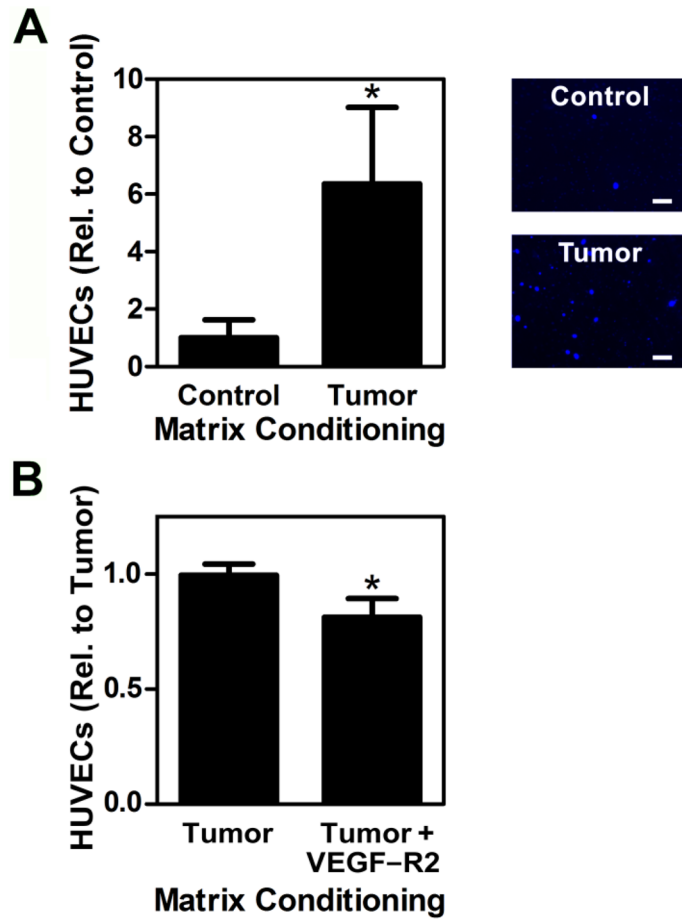


**Figure 4. Tumor ECM-induced VEGF secretion by stromal cells stimulates endothelial cell migration**

Media collected from 3T3-L1 cells cultured on tumor ECMs increased HUVEC migration in transwell migration assays relative to media collected from control ECMs, as measured via image analysis of DAPI-stained, fixed membranes following migration. Typical micrographs of migrated HUVECs stained with DAPI are shown at right. Scale bar = 20  $\mu\text{m}$  (A). Blockade of VEGF signaling using a VEGFR2/KDR peptide antagonist confirmed that greater VEGF levels secreted by stromal cells cultured on tumor ECMs contributed to changes in HUVEC migration (B). \* indicates  $p < 0.05$ .

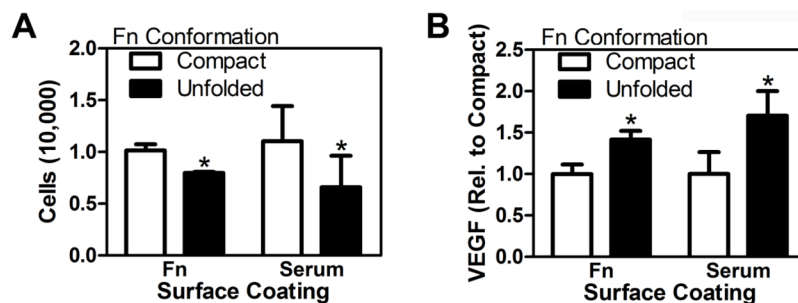


**Figure 5. Conducting polymer films to define the effect of Fn conformation on adhesion and VEGF secretion**

Oxidized (+1V) or reduced (-1V) PEDOT:PSS surfaces were coated with media containing either fibronectin (Fn) only, or 10% serum (containing Fn), to establish compact and partially unfolded conformations of adsorbed Fn, respectively. The number of 3T3-L1 cells per well adhered to unfolded Fn was decreased relative to compact Fn (A), while an opposite effect was detected for VEGF secretion (B) for both Fn and serum-coated devices. These differences were determined by image analysis of DAPI-stained fixed devices and VEGF ELISA followed by normalization to cell number. \* indicates  $p < 0.05$ .



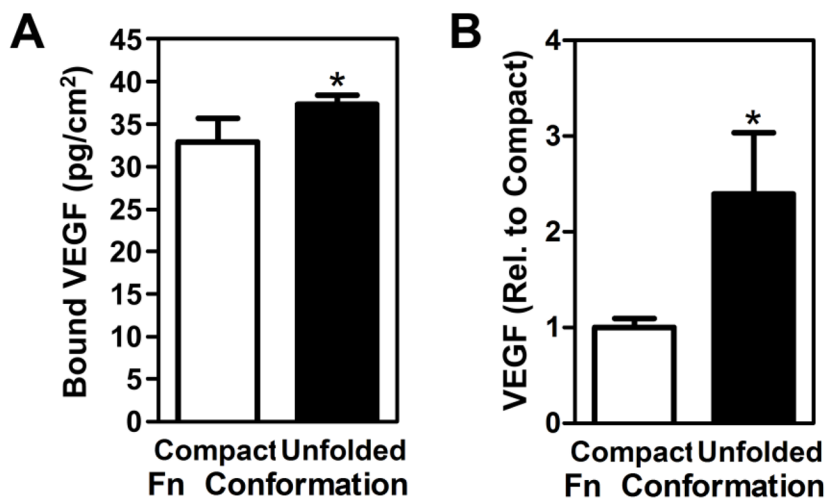


**Figure 6. Increased VEGF levels in response to partial Fn unfolding are not due to differential binding to Fn and are relevant to additional cell types**

Incubation of cell-free, serum-coated devices with recombinant VEGF followed by ELISA of non-bound VEGF in the media suggested that VEGF preferentially interacts with partially unfolded Fn and, hence, confirms that varied secretion rather than differential binding were responsible for the differences in VEGF levels detected above (A). Similar to 3T3-L1, human bone marrow-derived MSCs enhanced secretion of VEGF when seeded onto substrates with partially unfolded Fn relative to compact Fn as examined via VEGF ELISA followed by normalization to cell number (B). \* indicates  $p < 0.05$ .

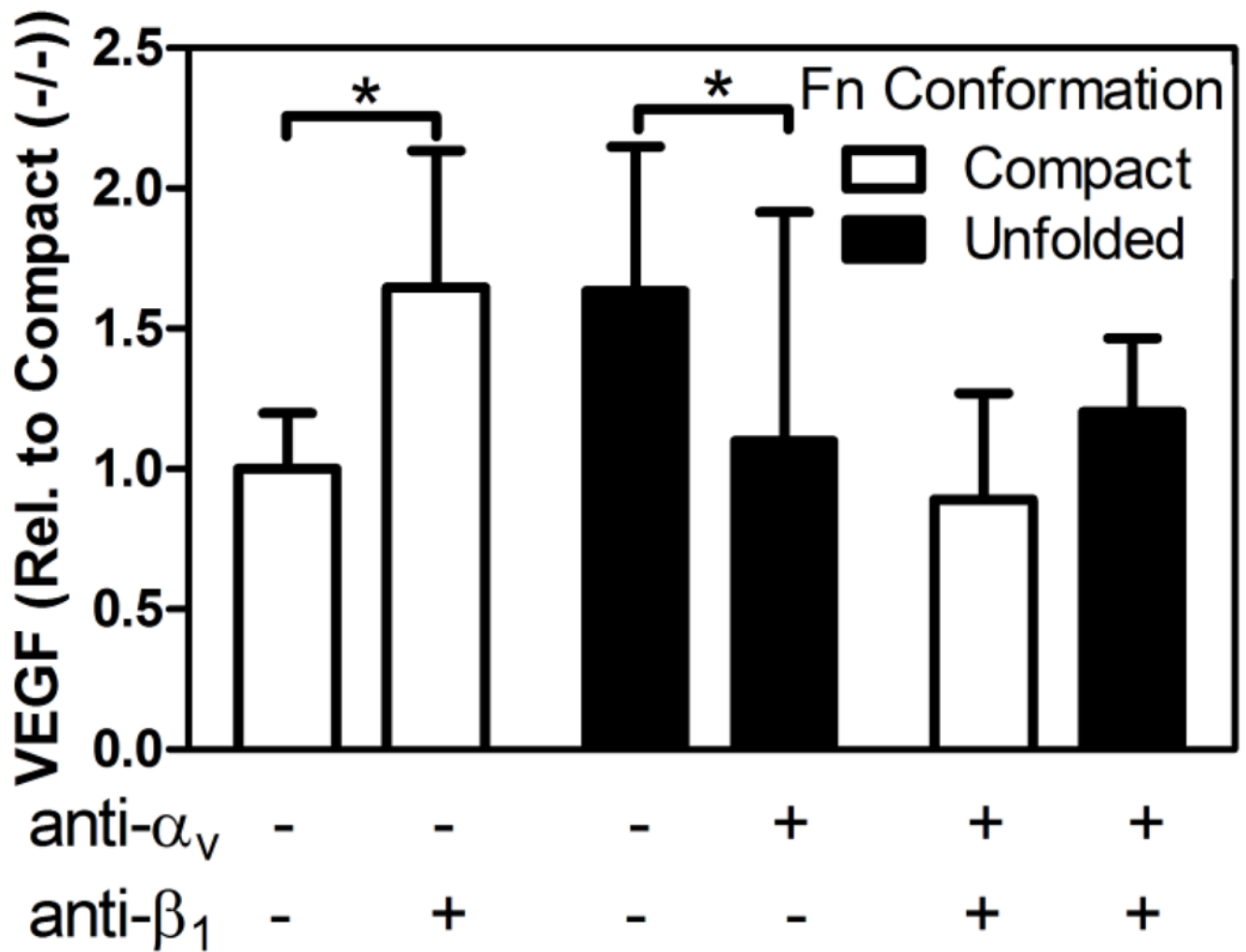


**Fig. 7. Varied Fn conformation regulates adhesion and VEGF secretion via altered integrin engagement**

Individual and combined blockade of synergy-dependent ( $\alpha_5\beta_1$ ) and -independent ( $\alpha_v\beta_3$ ) integrins via  $\beta_1$ - and  $\alpha_v$ -function blocking antibodies, respectively, suggested that  $\alpha_5\beta_1$  inhibits VEGF secretion of 3T3-L1 in response to compact Fn, which may be compensated by increased engagement of  $\alpha_v\beta_3$  (white bars). Additionally,  $\alpha_v\beta_3$  stimulates VEGF secretion in response to partially unfolded Fn, which is independent of  $\alpha_5\beta_1$  usage (black bars). \* indicates  $p < 0.05$ .